

Effective coupling of cyclotron autoresonance maser and “gyrotron” modes on a phase-synchronized electron beam

A. V. Saviolov,¹ V. L. Bratman,¹ A. D. R. Phelps,^{2,*} and S. V. Samsonov¹

¹*Institute of Applied Physics, Russian Academy of Sciences, 46 Ulyanov Street, Nizhny Novgorod 603600, Russia*

²*Department of Physics and Applied Physics, University of Strathclyde, Glasgow G4 0NG, Scotland, United Kingdom*

(Received 4 October 1999)

For a cyclotron resonance maser (CRM) with a helical axis-encircling electron beam, the possibility of a strong interaction between cutoff (gyrotron) and traveling Doppler-up-shifted (cyclotron autoresonance maser) modes, which are in resonance with the electrons at the same frequency, is demonstrated. This effect can be used in a CRM oscillator of a new type, where the feedback and the mode selectivity for the operating traveling mode are provided due to the excitation of the cutoff mode. According to both the theory and the experiment, such a scheme can provide an effective excitation of the traveling mode with negligibly low losses associated with the cutoff mode.

PACS number(s): 41.60.Cr

I. INTRODUCTION

The cyclotron autoresonance maser (CARM) [1,2] is a well-known variety of cyclotron resonance maser (CRM). Unlike the gyrotron [3], which is the most common variety of CRM, the main feature of the CARM is the coupling of electrons, which move along helical trajectories in a uniform magnetic field, with a rf wave propagating not perpendicularly but almost parallel to the magnetic field. Similar to the free-electron laser (FEL) [4], this fact along with a relatively large value of the longitudinal electron velocity provide a large Doppler upconversion of the electron oscillatory (cyclotron) frequency. At a fixed magnetic field, it allows the achievement of a higher frequency compared to the gyrotron.

Another important feature of the CARM is caused by two main types of electron bunching in this device. Actually, unlike a near-cutoff wave as used in the gyrotron, a traveling wave induces in the electron beam not only azimuthal but also axial bunching [5]. One should emphasize that these two mechanisms of the electron bunching result in opposite dynamic deviations of the electron energy from its value corresponding to the exact cyclotron resonance and, therefore, they can be mutually compensated. If the phase velocity of the wave is exactly equal to the speed of light, then the entire compensation takes place and cyclotron resonance is automatically maintained during the electron-wave interaction (autoresonance) [6]. According to the theory [1], for a high enough quality of the electron beam this effect can provide a high electron efficiency due to a prolonged resonant electron-wave interaction.

In spite of its advantages, the CARM is studied less often than the FEL and the gyrotron. The main reason is the relatively low efficiency obtained in most experiments [7–12]. Only in Ref. [13] was the achieved electron efficiency (26%) not lower than in the best FEL's and close to the theoretical

prediction for the ideal electron beam. This had been achieved, in particular, by improving the electron-beam formation, as well as by decreasing the sensitivity to the velocity spread due to shortening the region of electron-wave interaction. However, some features of the experiment [13] did not have a clear interpretation in Ref. [13]. The most important one was a significant difference between the radiation frequency and the eigenfrequency of the cavity. It was clear that the radiation frequency was close to the cutoff frequency of the TE_{2,1} mode. In principle, the axis-encircling electron beam used could excite this mode at the second cyclotron harmonic (large orbit gyrotron regime) [14]. The observed transverse structure of the output radiation, however, coincided with that for the operating TE_{1,1} mode. That is why in Ref. [13] the difference in frequency was attempted to be explained by an electron shift of the cavity eigenfrequency (a frequency pulling), although this explanation was not confirmed by later detailed simulations.

In this paper, a less obvious and more interesting explanation of the results of the experiment [13] is proposed. It is based on the fact that a thin helical electron beam provides an effective interaction between the CARM TE_{1,1} and “gyrotron” TE_{2,1} modes, which are excited at the same frequency but at various cyclotron harmonics, namely, at the fundamental and second harmonic. According to an analysis, in the experiment [13] the cavity used was occasionally closed for the gyrotron mode. Presumably, due to this fact this mode was also excited and then effectively scattered into the “CARM” mode on the electron beam. This effect can be considered, at least, as a way for spurious excitation in CARM's, as well as in large orbit gyrotrons. On the other hand, it seems attractive to use this effect for realization of a CRM oscillator of a new type. In such an oscillator, both modes are excited simultaneously. The “gyrotron” mode provides an effective feedback and selectivity whereas the operating CARM mode provides a high efficiency and output of radiation. According to the theory developed in this paper, the electron efficiency of this device can reach 40–60%. The work of Ganguly and Hirschfield [15] on radiation from spatiotemporally modulated electron beams is clearly relevant in this context.

*Present address: Physics and Applied Physics Department, University of Strathclyde, Glasgow G4 0NG, Scotland, UK. FAX: +44 (0)1415522891. Electronic address: a.d.r.phelps@strath.ac.uk

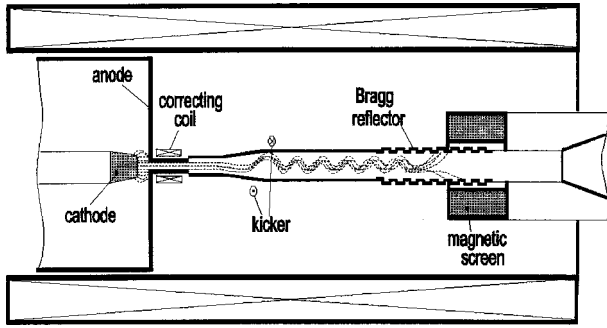


FIG. 1. Schematic of the CARM experiment [13].

In principle, the proposed scheme of a CRM oscillator is analogous to the sectioned, multiwave CRM based on the Doppler multiplication of the frequency [16]. In this device, a near-cutoff mode with some frequency, ω_1 , is excited in the first section and then, in the second section, it is scattered in a traveling wave with the frequency $\omega_2 = n\omega_1$. However, even for an ideal electron beam, the predicted efficiency of this device does not exceed 10%, while the length required for the interaction region is rather long. Another analogy is related to a quite novel idea of the gyro-TWT [17]. It is also based on coupling of the near-cutoff and traveling modes; however, the coupling is provided not by an electron beam but by a proper helical corrugation of the waveguide walls. One should mention also the work [18] in which a double resonance at the same frequency but at different harmonics is studied for the CRM with a conventional electron beam.

In Sec. II of this paper, results of the experiment in Ref. [13] are briefly discussed from the new point of view. Section III is devoted to an explanation of a possible mechanism for effective coupling of the near-cutoff and traveling modes on a phase-synchronized electron beam. In Sec. IV, a theory of the CRM oscillator, based on simultaneous excitation of the two modes at the same frequency, is developed. In Sec. V, results of a preliminary experiment, where such an oscillator has been specially realized, are given.

II. CARM EXPERIMENT

In the experiment in Ref. [13], a possibility of high-efficiency CARM operation was demonstrated (Fig. 1). A 500 keV/100 A operating electron beam with a pulse duration of 20 ns produced an output power of 13 MW at a frequency of about 38 GHz (the corresponding electron efficiency amounted to 26%). A thin rectilinear electron beam entered the operating cavity, being a piece of the circular waveguide terminated by two reflectors for the operating $TE_{1,1}$ wave, namely, a cutoff input narrowing and an output Bragg reflector. Inside the cavity (at its input), a magnetostatic kicker imparted transverse (rotary) momentum to the electrons. After having been kicked, the electrons were in cyclotron resonance with the forward traveling component of the operating $TE_{1,1}$ mode,

$$\omega \approx h v_z + \Omega. \quad (1)$$

Here ω is the frequency, h is the longitudinal (axial) wave number of the $TE_{1,1}$ mode, v_z is the longitudinal electron

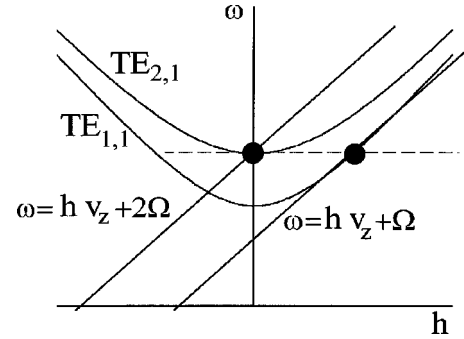


FIG. 2. Dispersion diagram for the fundamental CARM and second-harmonic gyrotron resonances at the same frequency.

velocity, $\Omega = eB/mc\gamma$ is the cyclotron frequency, and $\gamma = 1/\sqrt{1 - (v/c)^2}$ is the electron Lorentz factor.

In this experiment, some unexpected results were obtained. Namely, one could distinguish two different regimes of the CARM oscillations taking place at different values of the operating magnetic field. In the first regime, a radiation at a planned frequency close to 36 GHz, which was inside the feedback frequency band provided by the Bragg reflector, was observed. In the second regime, where the highest efficiency was achieved, the frequency of the output radiation was higher (of about 38 GHz), and it was out of the band of the Bragg reflector. Thus, at this frequency the feedback for the traveling $TE_{1,1}$ mode was not provided, whereas the power of the output radiation was 30–50% higher than in the first regime. It was important that in the second regime the radiation frequency was close to the cutoff frequency of the $TE_{2,1}$ mode, and this mode also could be in synchronism with electrons at the second cyclotron harmonic (Fig. 2):

$$\omega \approx 2\Omega. \quad (2)$$

It is necessary to note that such a situation is not too “exotic.” In CARM experiments, the grazing regime of the dispersion characteristics (Fig. 2) is often used for the operating transverse mode in order to avoid the “gyrotron” excitation of this mode at a lower frequency. Due to grazing, the cyclotron resonance for this mode has a rather wide frequency band. This fact facilitates the possibility for simultaneous achievement of the two synchronism conditions, Eqs. (1) and (2), at the same frequency.

In addition, in the experiment in Ref. [13] there was a significant difference in values of the output power, which were obtained in experiments with different types of Bragg reflectors. The rf power was significantly higher when the minimum radius of the reflector was smaller than the radius of the operating waveguide (analogous effects have been observed in CARM-oscillator experiments carried out at MIT [19]). In this case, the reflector provided almost 100% reflection and, therefore, a very high Q factor for the near-cutoff $TE_{2,1}$ mode. Certainly, it would be natural to suppose that the second-harmonic gyrotron operation of the $TE_{2,1}$ mode was obtained instead of the CARM operation of the $TE_{1,1}$ mode. However, measurements showed that the transverse structure of the output radiation corresponded to the CARM mode.

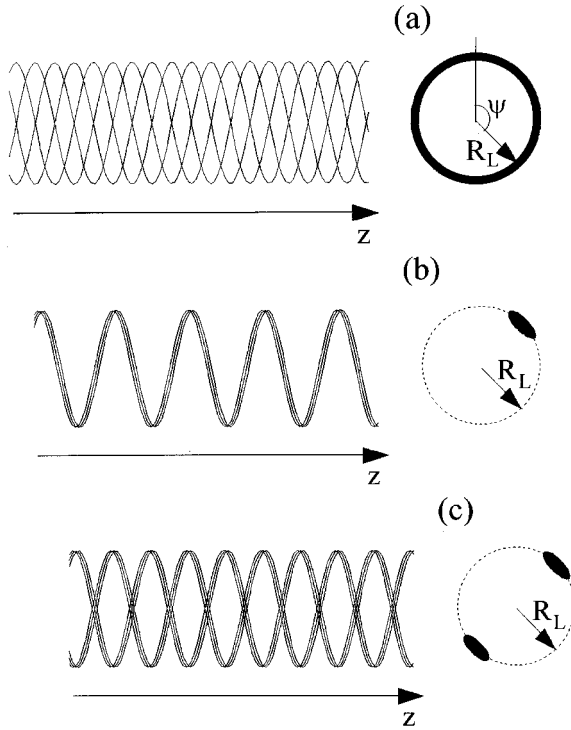


FIG. 3. Various types of electron beams: (a) hollow beam with homogeneous distribution of electrons over their gyrophases, (b) phase-synchronized helical beam, and (c) an artificial electron beam formed by two counterphased helices.

III. MECHANISM FOR COUPLING OF TRAVELING AND NEAR-CUTOFF MODES

A possible interpretation of the results obtained in Ref. [13] can be based on the effect of coupling of the traveling and near-cutoff modes (CARM and ‘gyrotron’ modes) on the electron beam. Such coupling can be effective, if the modes form electron bunches with spatial structures of the currents being not mutually orthogonal. This means that a mode should induce such perturbations in the electron beam that can excite the other mode. Let us consider an axis-circulating electron beam and introduce phases of an electron with respect to the CARM and gyrotron modes, θ_1 and θ_2 ,

$$\theta_1 = \omega t - hz - \psi, \quad \theta_2 = \omega t - 2\psi. \quad (3)$$

Here z is the longitudinal coordinate and Ψ is the angular coordinate of the particle (Fig. 3). The spatial structure of the electron-density perturbations (electron bunches), which are formed by a mode, is the interception of the electron beam with the surface of the constant phase corresponding to the mode. In the case of a hollow electron beam in the form of a cylinder of Larmor radius [Fig. 3(a)], when $0 \leq \Psi_0 < 2\pi$, the traveling $TE_{1,1}$ mode forms a rotating helix, $\Psi = \hat{\Psi}_0 + \omega t - hz$, with the period $L_w = 2\pi/h$ [Fig. 4(a)]. In the case of the near-cutoff $TE_{2,1}$ mode interacting with the electrons at the second cyclotron harmonic, it forms electron bunches being two oscillating ‘rods’ parallel to the longitudinal axis, $\Psi = \hat{\Psi}_0 + \omega t/2$ and $\Psi = \hat{\Psi}_0 + \pi + \omega t/2$. Here $\hat{\Psi}_0$ is the initial angular coordinate of the central electron of the bunches. Thus, in a hollow beam the modes form electron-density perturbations with completely different structures

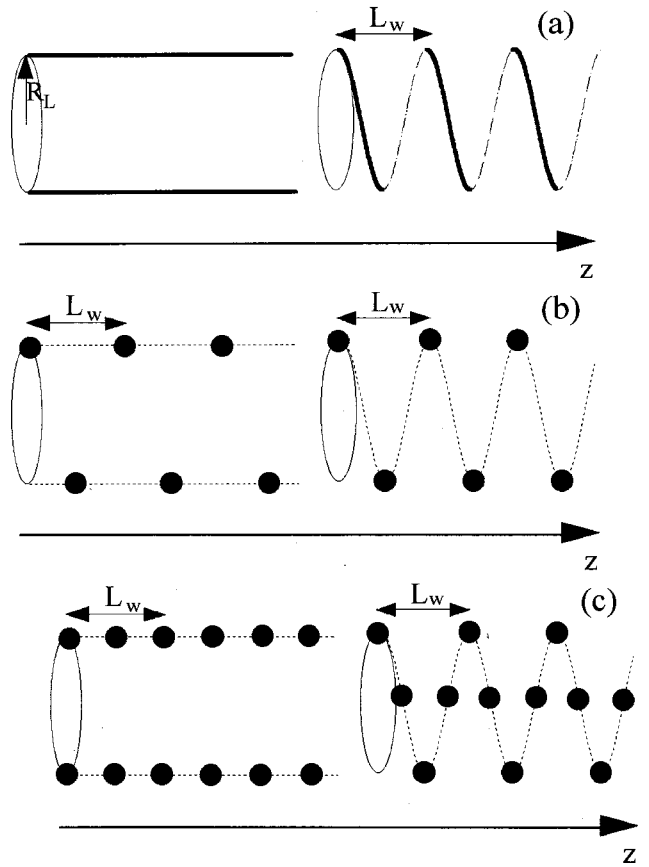


FIG. 4. Spatial structure of electron bunches formed by second-harmonic ‘gyrotron’ and CARM modes for hollow (a), helical (b), and two-helix (c) electron beams.

and, therefore, their interaction is very weak, though it is possible due to principally nonlinear effects [18].

However, in the experiment in Ref. [13] after the kicker the electron beam had a helical form [Fig. 3(b)]. Such a phase-synchronized beam, which consists of particles having the same initial gyrophases, can be considered as a fraction of the hollow beam. Therefore, the electron bunches in the helical beam represent some fractions of corresponding bunches in the hollow beam. Let us consider a very thin helical beam: $0 \leq \psi_0 \leq \Delta\psi_0$ and $\Delta\psi_0 \leq \pi$. Unlike the hollow electron beam, the spatial structures of the electron bunches in the helical beam are periodical and discrete. Actually, the initial angular coordinate of the central electrons of the bunches changes in time as $\hat{\psi}_0 = \omega t$. For such a beam, the central electron enters the interaction region periodically with the time interval $\Delta t = 2\pi/\omega$. This corresponds to the distance between bunches $\Delta L = 2\pi v_z/\omega$. According to the resonance conditions Eqs. (1) and (2), $\omega \approx 2hv_z$. Thus, in the helical beam both modes form electron bunches, which are periodical parts of the corresponding bunches in the hollow beam with the period

$$\Delta L = \pi/h = L_w/2. \quad (4)$$

As demonstrated in Fig. 4(b), for the helical beam the spatial structures of electron-density perturbations are just the same for both the ‘gyrotron’ and the CARM modes. It means that these modes can be effectively coupled on the beam. The

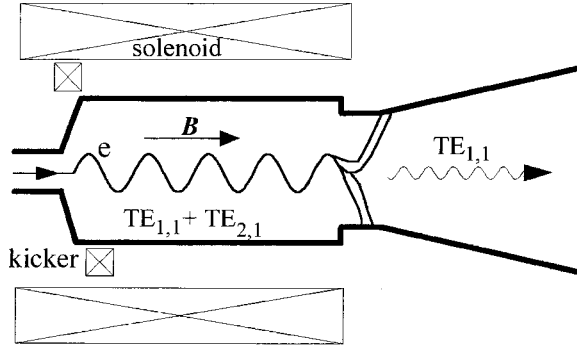


FIG. 5. Schematic of CRM oscillator based on simultaneous excitation of “gyrotron” and CARM modes.

same result can be obtained also for the excitation of the “gyrotron” mode at any higher cyclotron harmonic.

One should emphasize again that the possibility of the effective interaction between the CARM and the “gyrotron” modes is a result of the helical form of the electron beam (phase-synchronized gyrorotation of all the electrons). In the hollow beam with uniform initial distribution of particles over gyro-phases, the interaction is very weak. In order to demonstrate the transition from the helical beam to the hollow one, let us consider some artificial beam in the form of two counterphased helices [Fig. 3(c)]. As compared to the helical beam, the second helix leads to the appearance of “new” bunches. For both modes one should supplement the periodical bunch systems shown in Fig. 4(b) with the corresponding counterphased systems [Fig. 4(c)]. It is important that the “new” bunches, which correspond to one of the modes, are in the opposite phases with respect to the “new” bunches corresponding to the other mode. Therefore, the mode coupling on this beam is weak.

IV. CRM BASED ON SIMULTANEOUS EXCITATION OF GYROTRON AND CARM MODES

The effect of coupling of the “gyrotron” and CARM modes on a helical electron beam can be considered, at least, as a possible factor for excitation of spurious modes in various types of CRM. At the same time, this effect can be used for realization of an attractive scheme of a CRM oscillator with a simple gyrotron-type cavity. For instance, it can be a piece of cylindrical waveguide with cutoff narrowings at the input and output (Fig. 5). Such a cavity is closed for the near-cutoff “gyrotron” mode. Correspondingly, the quality of this mode is very high and defined basically by Ohmic losses in the cavity walls. At the same time, the slight output narrowing practically does not reflect the traveling CARM mode. Therefore, this cavity provides an effective feedback for the “gyrotron” mode only. However, if a helical electron beam is used and the synchronism conditions Eqs. (1) and (2) are simultaneously satisfied, then the effective excitation of the CARM mode can be caused by the excitation of the “gyrotron” mode and coupling of the modes on the beam. In this oscillator, the operating channel of the rf power output is provided by the CARM mode. The “gyrotron” mode is needed in order to provide feedback and the proper electron bunching for the CARM mode only; its own power is dissipated in the cavity walls. One should note some advantages

of this scheme of the feedback for the traveling wave, which propagates almost parallel to the cavity axis. Along with simplicity of the microwave system, this scheme solves the problem of the mode control, which is very important for CARM’s. The stable generation of the “gyrotron” mode can fix the frequency of the operating CARM mode.

A. Equations of the mode coupling on the helical electron beam

Let us study simultaneous excitation of the CARM and “gyrotron” modes at the same frequency in a cavity shown in Fig. 5. The following expressions describe the structures of azimuthally rotating modes:

$$E_+ = ike^{i\psi} \left\{ \frac{\partial J_1(gr)}{\partial(gr)} \text{Im}(A_1 e^{i\theta_1}) + \frac{iJ_1(gr)}{gr} \text{Re}(A_1 e^{i\theta_1}) \right\},$$

$$B_+ = i \frac{h}{k} E_+, \quad B_z = gJ_1(gr) \text{Re}(A_1 e^{i\theta_1})$$

for the traveling $TE_{1,1}$ mode, and

$$E_+ = ik \sin(\pi z/L) e^{i\psi} \left\{ \frac{\partial J_2(kr)}{\partial(kr)} \text{Im}(A_2 e^{i\theta_2}) + \frac{iJ_2(kr)}{kr} \text{Re}(A_2 e^{i\theta_2}) \right\},$$

$$B_+ = 0, \quad B_z = k \sin(\pi z/L) J_2(kr) \text{Re}(A_2 e^{i\theta_2})$$

for the near-cutoff $TE_{2,1}$ mode. Here $E_+ = E_x + iE_y$, $B_+ = B_x + iB_y$, r and ψ are polar coordinates, $k = \omega/c$, J_n is the Bessel function of the n th order, g_1 is the transverse wave number of the $TE_{1,1}$ mode (for the $TE_{2,1}$ mode, $g_2 \approx k$), L is the cavity length, and the electron phases with respect to the modes, θ_1 and θ_2 , are defined by Eqs. (3). Here we have assumed that the cavity provides a high quality for the “gyrotron” $TE_{2,1}$ mode and fixes its longitudinal structure and the frequency. For simplicity, we have assumed the sinusoidal distribution so that the amplitude A_2 does not depend on the coordinate, z . As for the CARM $TE_{1,1}$ mode, its Q factor is low, and its longitudinal structure, $A_1 = A_1(z)$, is defined basically by its interaction with the helical electron beam having been bunched by the “gyrotron” mode.

In order to describe the interaction of electrons with the two modes, we shall use a modification of the well-known averaged (over fast cyclotron rotation) equations [1]. Let us represent the electron Lorentz factor as $\gamma = \gamma_0(1 + w_1 + w_2)$, where w_1 and w_2 describe the energy exchange between the electron and the two modes (CARM and “gyrotron” modes, respectively) and satisfy the following equations:

$$\frac{dw_1}{d\zeta} = -\chi_1 \text{Im}(a_1 e^{i\theta_1}),$$

$$\frac{dw_2}{d\zeta} = -\chi_2 \sin(\pi \zeta/L) \text{Im}(a_2 e^{i\theta_2}).$$

Here $\zeta = kz$ is the normalized longitudinal coordinate, $a_{1,2} = eA_{1,2}/mc^2 \gamma_0$, $\chi_1 = p_{\perp}/2p_z$ and $\chi_2 = p_{\perp}^2/2p_z$ are the cou-

pling coefficients, $p_{\perp,z} = \gamma v_{\perp,z} / \gamma_0 c$ are the normalized components of the electron momentum, and $\hat{L} = kL$ is the normalized cavity length. Then, we take into account that the change in longitudinal momentum of a particle is caused by its interaction with the CARM mode only and approximately described by the well-known integral [6,1]

$$p_z - \beta_{z_0} = w_1 / \beta_{\text{ph}}. \quad (6)$$

Here $\beta_{\text{ph}} = k/h$ and $\beta_{z_0} = v_{z_0}/c$ are the phase velocity of the CARM mode and the initial longitudinal electron velocity normalized by the speed of light. This allows the representation of the equations for the electron phases with respect to the modes in the following form:

$$\begin{aligned} \frac{d\theta_1}{d\zeta} &= \frac{-\delta_1 - (1 - \beta_{\text{ph}}^{-2})w_1 - w_2}{p_z} - F, \\ \frac{d\theta_2}{d\zeta} &= \frac{-\delta_2 - w_1 - w_2}{p_z} - 2F. \end{aligned} \quad (7)$$

Here $\delta_1 = 1 - \beta_{z_0}/\beta_{\text{ph}} - \Omega_0/\omega$ and $\delta_2 = 1 - 2\Omega_0/\omega$ are the mismatches of the cyclotron resonance for both the modes, Ω_0 is the initial electron cyclotron frequency, and F describes the so-called ‘‘forced’’ electron bunching:

$$\begin{aligned} F &= \hat{\chi}_1 \text{Re}(a_1 e^{i\theta_1}) + \hat{\chi}_2 \sin(\pi\zeta/\hat{L}) \text{Re}(a_2 e^{i\theta_2}) \\ &+ eB_z/mc\gamma_0\omega p_z, \end{aligned}$$

where $\hat{\chi}_1 = (1/\beta_z - 1/\beta_{\text{ph}})/2p_z$, $\hat{\chi}_2 = 1/2\beta_z$, and B_z is the sum of the longitudinal components of the magnetic fields of the modes. The initial conditions for Eqs. (7) have the form

$$\theta_1(0) = \omega t_0 - \psi_0, \quad \theta_2(0) = \omega t_0 - 2\psi_0, \quad (8)$$

where the entering times, t_0 , and the initial angular phases of particles, ψ_0 , are homogeneously distributed within the intervals $0 \leq \omega t_0 < 2\pi$ and $0 \leq \psi_0 \leq \Delta\psi_0$, respectively. Here $\Delta\psi_0$ is the phase thickness of the electron beam. For the ideal helical beam $\Delta\psi_0 = 0$ and for the hollow beam $\Delta\psi_0 = 2\pi$ (Fig. 3).

A slow temporal evolution of the ‘‘gyrotron’’ mode amplitude during its interaction with the electron beam is described by the equation

$$\frac{da_2}{d\tau} + \frac{a_2}{2Q_2} = i \frac{G_2}{\hat{L}} \int_0^{\hat{L}} \sin(\pi\zeta/\hat{L}) \langle \chi_2 e^{-i\theta_2} \rangle_{t_0, \psi_0} d\zeta. \quad (9)$$

Here $\tau = \omega t$, Q_2 is the quality of this mode, and $\langle \rangle_{t_0, \psi_0}$ indicates averaging over initial parameters t_0 and ψ_0 of all electrons. As for the CARM mode, the cavity is assumed to provide no feedback for this mode. In this situation, the excitation of this mode is described by the spatial equation for a waveguide mode,

$$\frac{da_1}{d\zeta} = iG_1 \langle \chi_1 e^{-i\theta_1} \rangle_{t_0, \psi_0}, \quad (10)$$

with the zero amplitude at the cavity input,

TABLE I. Parameters of calculations.

Cyclotron harmonics	first and second
Transverse modes	TE _{1,1} and TE _{2,1}
Frequency (GHz)	37.8
Beam voltage (kV)	500
Beam current (Å)	50
Cavity radius (cm)	0.39
Length of the cavity (cm)	8
Q factor of the cavity	~3000

$$a_1(\zeta=0) = 0. \quad (11)$$

In Eqs. (9) and (10) the factors of excitation are defined by the expressions

$$G_1 = \frac{2I\beta_{\text{ph}}(1 - \beta_{\text{ph}}^{-2})}{I_A N_1 \gamma_0}, \quad G_2 = \frac{8I}{I_A N_2 \gamma_0},$$

where I is the electron current, $I_A = mc^3/e$, and $N_{1,2}$ are the wave norms.

Thus, quasistationary equations (5)–(11) describe simultaneous excitation of the ‘‘gyrotron’’ and CARM modes at a frequency which is fixed by the ‘‘gyrotron’’ mode. Efficiencies of the interaction of the electron beam with each of the modes are described by the expressions

$$\eta_{1,2}(\tau) = \frac{-\langle w_{1,2}(\tau) \rangle_{t_0, \psi_0}}{1 - \gamma_0^{-1}},$$

which represent the averaged (over all electrons) parts of the initial kinetic electron energy passed to each of the modes.

B. Results of simulations

In simulations we study a CRM with a configuration which is similar to the experiment in Ref. [13] (Table I), but with a slightly modified cavity of a gyrotron type (Fig. 5). The quality of the cavity for the ‘‘gyrotron’’ TE_{2,1} mode is defined by its Ohmic losses in the copper walls. Calculations show that in a wide range of the parameters (operating electron-beam current, electron pitch factor, quality of the cavity) it is possible to provide regimes with a very effective excitation of the CARM mode [Figs. 6(a) and 7]. In these regimes, a very small part of the electron energy is lost for excitation of the ‘‘gyrotron’’ mode. The electron efficiency, which corresponds to the interaction with this mode, η_2 , is at least lower than 1% [Figs. 6(b) and 7]. At the same time, at a sufficiently high oscillatory component of the initial electron velocity, $\beta_{\perp_0} = v_{\perp_0}/c = 0.60 - 0.65$, the electron efficiency, corresponding to the excitation of the operating CARM mode, can be as high as 40–60%.

According to quasistationary (fixed-frequency) calculations, this type of CRM operation is stable in time. Figure 8(a) illustrates the temporal dynamics of the oscillator as compared with the case of a hollow electron beam, when the CARM-mode excitation is not effective [Fig. 8(b)]. In the last case, simulations predict, after quite a long time, $\tau \sim Q$, a low-efficiency operation of the ‘‘gyrotron’’ mode with temporal modulations of its power. The modulations are

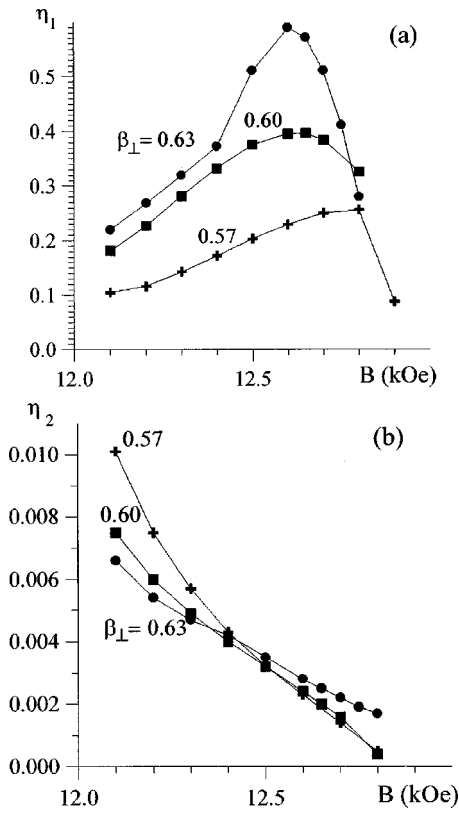


FIG. 6. CRM based on simultaneous excitation of “gyrotron” and CARM modes. Efficiency of the energy exchange with the operating CARM mode, η_1 (a) and the part of electron energy passed to the “gyrotron” mode, η_2 (b) vs the magnetic field B at various initial oscillatory electron velocity, $\beta_{\perp 0}$.

caused by overloading the mode, as its quality is so high that the operating current significantly exceeds the starting current for this mode. However, for the helical electron beam, the CARM-mode excitation results in the appearance of a

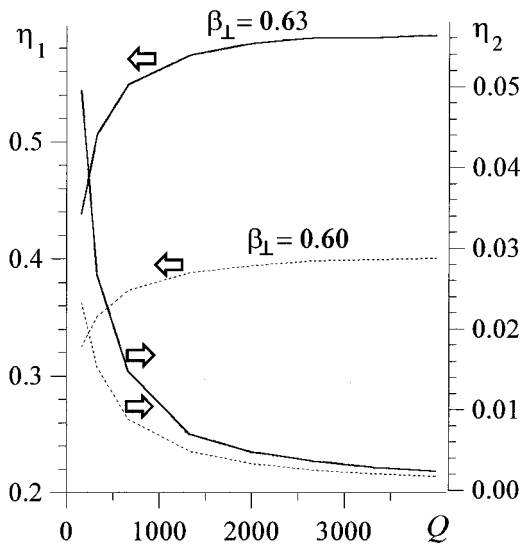


FIG. 7. Efficiency of the energy exchange with the operating CARM mode, η_1 , and the part of electron energy passed to the “gyrotron” mode, η_2 , vs the cavity quality for the near-cut-off mode, Q , at the optimal magnetic field and various initial oscillatory electron velocity, $\beta_{\perp 0}$.

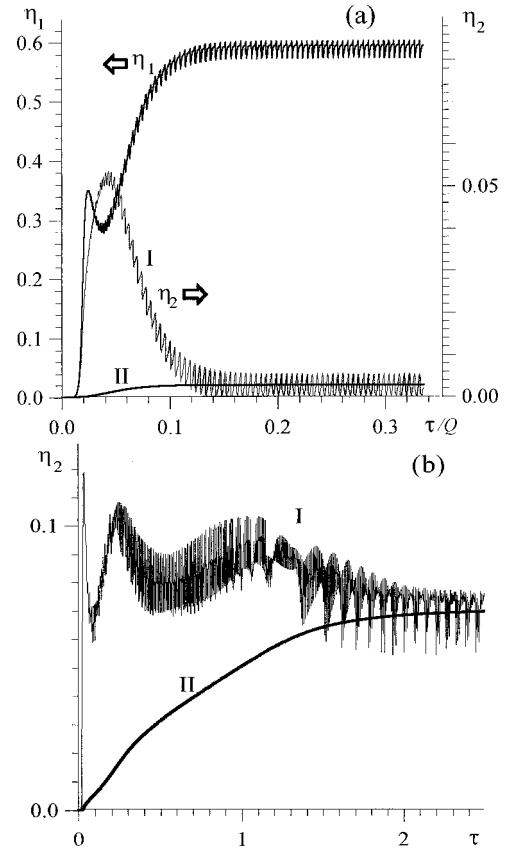


FIG. 8. Temporal dynamics of excitation of the CARM and “gyrotron” modes at the optimal magnetic field (a) and excitation of the “gyrotron” mode by the hollow electron beam, when the mode coupling is absent (b).

very effective channel for the power output. This looks like a decrease of the quality with the duration of the transient process significantly decreasing, and the output power being quite stable in time [Fig. 8(a)]. However, one should take into account that if the quality of the cavity is high enough, then the single-frequency generation of the “gyrotron” mode can be unstable (its frequency is not fixed) [20]. Thus, in principle, the problem of the temporal stability needs an additional analysis on the basis of the multifrequency theory.

The above simulations have been done for an ideal helical beam with “zero” thickness ($\Delta\psi_0=0$). As has been preliminarily demonstrated in Sec. III, the increase of the phase thickness, $\Delta\psi_0$, weakens the coupling of the modes. Figure 9 illustrates the transition from the ideal helical beam ($\Delta\psi_0=0$) to the hollow one ($\Delta\psi_0=2\pi$). While the beam is not too thick ($\Delta\psi_0<\pi/2$), the sensitivity to spread in the initial angular phase is quite weak. The further increase of the thickness leads to the decrease of the power generated by the CARM mode and, simultaneously, to the increase of the part of the electron energy which is lost due to the excitation of the “gyrotron” mode.

C. Discussion

The proposed method of the CARM-mode excitation is very effective, because the predicted efficiency of the energy exchange between the electron beam and the CARM mode is at least twice as high as theoretical limits for the simplest

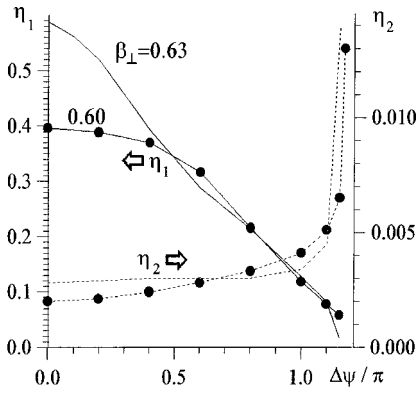


FIG. 9. Efficiencies of energy exchange between electron beam and the CARM and “gyrotron” modes, η_1 and η_2 , vs the phase thickness of the electron beam at the optimal magnetic field.

schemes of the CARM oscillator [1]. One could point out three main factors, which cause such high efficiency. The first one discussed in Sec. III is caused by the strong interaction between CARM and “gyrotron” modes in a thin helical beam because these modes induce the same perturbations in the beam. The second factor is that, in fact, the proposed oscillator operates as an amplifier for the CARM mode. It amplifies perturbations in the electron beam, which are induced by the “gyrotron” mode. It is known (see, e.g., Ref. [1]) that, as compared to oscillators, amplifiers provide higher efficiencies due to a “better” longitudinal structure of the amplified wave.

The third factor, which provides the high efficiency, could be understood from Fig. 10, which illustrates the energy ex-

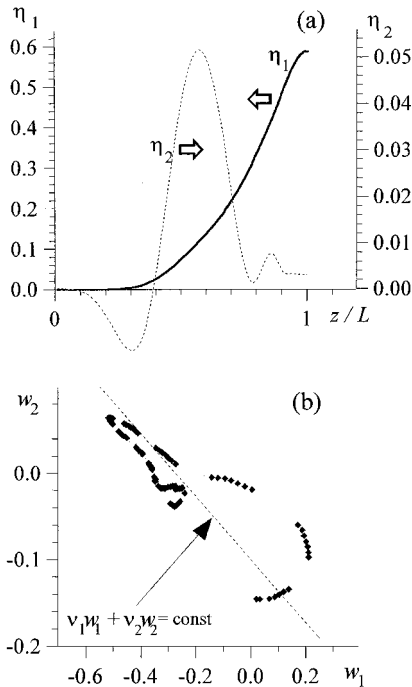


FIG. 10. The stationary stage of the CRM operation at the optimal magnetic field. Efficiencies of energy exchange between electron beam and the CARM and “gyrotron” modes, η_1 and η_2 , vs the longitudinal coordinate (a). Distribution of changes in electron energy, corresponding to the CARM and “gyrotron” modes, w_1 and w_2 , at the output of the interaction region (b).

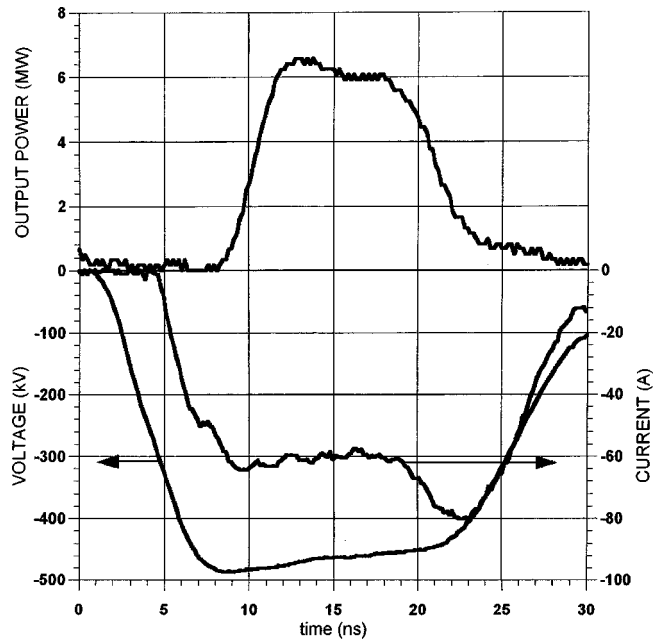


FIG. 11. Oscilloscope traces of voltage, current, and output microwave power for CRM based on simultaneous excitation of near-cutoff and traveling modes.

change between the modes at the stable stage of the optimal regime (the regime of the highest CARM efficiency, η_1). It is seen from Fig. 10(a) that in the first half of the interaction region the beam passes the energy mainly to the “gyrotron” mode. At the second half, the CARM mode takes almost the whole energy of the “gyrotron” mode. Thus, the suppression of the “gyrotron” mode increases the efficiency, η_1 , because it leads to the decrease of the energy losses, η_2 , which are spent for the excitation of this mode. At the same time, as follows from the analysis of Eq. (7) for the electron phase with respect to the CARM mode, the energy exchange between the modes is very effective. Within the framework of the approximation of the so-called inertial bunching [1] this equation can be reduced to the following simplified form:

$$\frac{d\theta_1}{d\zeta} \approx \frac{-\delta_1 - v_1 w_1 - v_2 w_2}{p_z} \quad (12)$$

Here $v_1 = 1 - \beta_{ph}^{-2}$ and $v_2 = 1$ are the coefficients of the inertial electron bunching, which are induced by CARM and “gyrotron” modes, respectively. This equation shows that a particle can effectively reradiate the rf power of the “gyrotron” mode into the CARM mode and, simultaneously, keeps the synchronism with the CARM mode. Really, if a particle takes back some energy, Δw_2 , from the “gyrotron” mode and, simultaneously, gives to the CARM mode the energy $\Delta w_1 = -\Delta w_2 v_2 / v_1$, then the particle does not lose its synchronism with the CARM mode. If the phase velocity of the CARM mode is close to the speed of light, $\beta_{ph} \sim 1$, then $|\Delta w_1| \gg |\Delta w_2|$. This means that high-power radiation of the CARM mode can be compensated for by a low-power absorption of the energy of the “gyrotron” mode. This effect is illustrated by Fig. 10(b), which shows the distribution of electrons over their changes in the energy, w_1 and w_2 , at

the output of the interaction region. It is seen that most particles are placed close to a line $v_1 w_1 + v_2 w_2 = \text{const}$.

V. EXPERIMENTAL REALIZATION OF THE CRM OSCILLATOR BASED ON SIMULTANEOUS EXCITATION OF TRAVELING AND NEAR-CUTOFF MODES

In order to clearly confirm the mechanism discussed above of the interaction between a second-harmonic gyrotron and a CARM mode, an experiment similar to that described in Sec. II was performed. A thin helical electron beam encircling the axis was produced using almost the same electron-optical system and was injected into the same 60-mm-long section of circular waveguide 7.7 mm in diameter having a 37.8-GHz cutoff frequency for the $TE_{2,1}$ mode. Unlike the experiment in Ref. [13], the cavity was terminated at its output not by a Bragg reflector but by a section of a smooth circular waveguide with smaller diameter 7.1 mm having 41-GHz cutoff frequency for the $TE_{2,1}$ mode (Fig. 5). Thus, the “cold” microwave feedback for the $TE_{1,1}$ mode was eliminated while a high- Q cavity for a second-harmonic gyrotron was provided.

As a result of the experiment, microwave radiation at a frequency of 40 ± 1 GHz having a mode pattern corresponding to the $TE_{1,1}$ mode was observed. The maximum output power was measured for an axial magnetic field of 11.0–11.3 kG and an electron pitch factor of about 1. The electron beam voltage, current, and output microwave power amounted to 460 kV, 60 A, and 6 MW, respectively (Fig. 11), which corresponded to 22% electronic efficiency (pre-

sumably, the slightly lower efficiency than in the experiment in Ref. [13] can be explained by the lower value of the electron current).

In addition, an experiment with the same cavity but terminated by the Bragg reflector was repeated. The reflector has grooves with a minimum and maximum diameter of 7.1 and 8.5 mm, respectively, and effectively reflected the $TE_{1,1}$ mode within a frequency band of 35–36 GHz. In this case both regimes of oscillations were observed again. At lower magnetic fields (10.3–10.5 kG) the “pure” CARM operation at 35.5-GHz frequency with an output power of nearly 4 MW was detected. At higher magnetic field the second regime with parameters close to those described above dominated. When the Bragg reflector had been substituted with a section of a smooth waveguide having the same diameter as the cavity, the output microwave had about five times smaller power, shorter pulse duration, and was unstable from shot to shot.

Thus, both the theory developed and the experiment described demonstrate the possibility of highly efficient operation of a cyclotron resonance oscillator at a Doppler-upshifted frequency without providing a special microwave feedback.

ACKNOWLEDGMENTS

This research is supported by the Russian Foundation for Fundamental Research, Grants No. 98-02-17068 and 99-02-16361, and by the United Kingdom DERA.

-
- [1] M. I. Petelin, *Radiophys. Quantum Electron.* **17**, 686 (1974); V. L. Bratman, N. S. Ginzburg, and M. I. Petelin, *Opt. Commun.* **30**, 409 (1979); V. L. Bratman, N. S. Ginzburg, G. S. Nusinovich, M. I. Petelin, and P. S. Strelkov, *Int. J. Electron.* **51**, 541 (1981); V. L. Bratman, G. G. Denisov, N. S. Ginzburg, and M. I. Petelin, *IEEE J. Quantum Electron.* **QE-19**, 282 (1983).
- [2] J. L. Vomvoridis, *Int. J. Electron.* **53**, 555 (1982); P. Sprangle, C.-M. Tang, and P. Serafim, *Nucl. Instrum. Methods Phys. Res. A* **250**, 361 (1986).
- [3] A. V. Gaponov, M. I. Petelin, and V. K. Yulpatov, *Radiophys. Quantum Electron.* **10**, 686 (1967); J. L. Hirshfield and V. L. Granatstein, *IEEE Trans. Microwave Theory Tech.* **MTT-25**, 522 (1977).
- [4] J. M. J. Madey, *J. Appl. Phys.* **42**, 1906 (1971); W. B. Colson, *Phys. Lett.* **64A**, 190 (1977).
- [5] A. V. Gaponov, *Zh. Eksp. Teor. Fiz.* **39**, 326 (1960) [*Sov. Phys. JETP* **12**, 232 (1960)].
- [6] A. A. Kolomensky and A. N. Lebedev, *Dokl. Akad. Nauk SSSR* **145**, 1259 (1962) [*Sov. Phys. Dokl.* **7**, 745 (1963)]; V. Ya. Davydovsky, *Zh. Eksp. Teor. Fiz.* **43**, 886 (1962) [*Sov. Phys. JETP* **16**, 629 (1963)].
- [7] I. E. Botvinnik, V. L. Bratman, A. B. Volkov, N. S. Ginzburg, G. G. Denisov, B. D. Kol'chugin, M. M. Ofitserov, and M. I. Petelin, *Pis'ma Zh. Eksp. Teor. Fiz.* **35**, 418 (1982) [*JETP Lett.* **35**, 516 (1982)].
- [8] G. Bekefi, A. DiRienzo, C. Leibovitch, and B. G. Danly, *Appl. Phys. Lett.* **54**, 1302 (1989).
- [9] A. W. Fliflet, R. B. McCowan, C. A. Sullivan, D. A. Kirkpatrick, C. H. Gold, and W. M. Manheimer, *Nucl. Instrum. Methods Phys. Res. A* **285**, 233 (1989).
- [10] M. Caplan, B. Kulke, G. A. Westenskow, D. B. McDermott, and N. C. Luhmann, Lawrence Livermore National Laboratory Report No. UCRL-53689-90, 1990.
- [11] S. Alberti, B. G. Danly, G. Gulotta, E. Giguët, T. Kimura, W. L. Menninger, J. L. Rullier, and R. J. Temkin, *Phys. Rev. Lett.* **71**, 2018 (1993).
- [12] S. J. Cooke, S. N. Spark, A. W. Cross, W. He, and A. D. R. Phelps, in *Proceedings of the 18th International Conference on Infrared and Millimeter Waves, Sendai, Japan, 1994* (International Society of Optical Engineers, SPIE, Bellingham, WA, 1997), p. 427; S. J. Cooke, A. W. Cross, W. He, and A. D. R. Phelps, *Phys. Rev. Lett.* **77**, 4836 (1996).
- [13] V. L. Bratman, G. G. Denisov, B. D. Kolchugin, S. V. Samsonov, and A. B. Volkov, *Phys. Rev. Lett.* **75**, 3102 (1995).
- [14] W. Lawson, W. W. Destler, and C. D. Striffler, *IEEE Trans. Plasma Sci.* **13**, 444 (1985).
- [15] A. Ganguly and J. Hirshfield, *Phys. Rev. E* **47**, 4364 (1993).
- [16] A. F. Aleksandrov, S. Yu. Galuso, V. I. Kanavets, V. A. Kubarev, S. A. Sokolov, and V. A. Cherepenin, *Radiotekh. Elektron. (Moscow)* **29**, 1788 (1984).
- [17] G. G. Denisov and S. J. Cooke, in *Digest of the 21st International Conference on Infrared and Millimeter Waves, Berlin, 1996* (Humbolt Universität zu Berlin, Berlin, 1996), p. AT1;

- G. G. Denisov, V. L. Bratman, A. D. R. Phelps, and S. V. Samsonov, *IEEE Trans. Plasma Sci.* **26**, 508 (1998); G. G. Denisov, V. L. Bratman, A. W. Cross, W. He, A. D. R. Phelps, K. Ronald, S. V. Samsonov, and C. G. Whyte, *Phys. Rev. Lett.* **81**, 5680 (1998).
- [18] G. Nusinovich and J. Zhao, *Phys. Rev. E* **58**, 1002 (1998).
- [19] B. G. Danly (private communication).
- [20] N. S. Ginzburg, N. A. Zavolsky, G. S. Nusinovich, and A. S. Sergeev, *Izv. Vyssh. Uchebn. Zaved., Radiofiz.* **XXIX**, 106 (1986).